Int. J. Electrochem. Sci., 16 **(2021)** Article ID: 210747, doi: 10.20964/2021.07.49

International Journal of
ELECTROCHEMICAL
SCIENCE
www.electrochemsci.org

Synergistic effect of dispersant and wetting reagent on wettability, thermal Stability and electrochemical properties of PVDF-coating polyethylene separator for lithium-ion batteries

Ji Yan[*], *Xiao-Kai Ma, Min-Yun Wang, Jun-Peng Ni, Ke-Zheng Gao, Yong Zhang, Li-Zhen Wang*[*]

School of Materials and Chemical Engineering, Zhengzhou University of Light Industry, Zhengzhou 450001, Henan, PR China
[*]E-mail: jiyan@zzuli.edu.cn, wlz@zzuli.edu.cn

Received: 2 February 2021 / *Accepted:* 10 March 2021 / *Published:* 31 May 2021

Aim to improve the physical and related electrochemical properties of surface-coating separator, in this article, two kinds of dispersant and four kinds of wetting reagent were utilized to investigate their synergistic effect on the PVDF-coated polyethylene (PE) separator. After characterized with contact angle, slurry viscosity, electrolyte uptake ability and high-temperature baking, the PVDF-coating PE separator prepared under assistance of perfluorinated octylic acid sodium as dispersant and ethylene bis stearic acid amide as wetting reagent was assembled into MCMB//Li asymmetric battery. The results show that the PVDF-coating PE separator possesses reduced contact angle, improved electrolyte uptake ability and enhanced thermal shrinkage stability. Furthermore, the assembled battery with PVDF-coating PE separator can provide 304.2 mAh g^{-1} of specific capacity with capacity retention reaching 93.2% after 50 cycles at 0.5C. The rate-recovering efficiency can back up to 95.1% at 0.1C after cycling at various rates. In comparison with bare PE, the battery with PVDF-coating PE separator demonstrates improved rate property and enhanced cycling stability. Even after 60% over-charging for 20 cycles at 0.2C, the battery with optimal condition separator can possess 84.9% of its initial specific capacity at 0.1C, strongly proven the superior over-charging tolerance. The synergistic effect between dispersant and wetting reagent can be utilized efficiently in preparation of high-quality separator for lithium ion batteries.

Keyword: Synergistic effect; Separator; Electrochemical properties; Lithium ion batteries.

1. INTRODUCTION

The ever-growing environmental pollution has aroused researchers to find suitable green energy to replace traditional fossil fuel such as coal and petrol. Among enormous candidates, lithium ion battery has made huge commercial success and has been widely utilized in our daily life including 3C electronic device, mobile, as well as electric vehicle [1]. As one of important components in lithium ion battery,

the performance of separator has attracted tremendous enthusiasm from industrial and scientific researchers since it severely affects the safety of lithium ion batteries, which is the most harmful issue in large-scale application of the battery in the field of energy storage and electronic vehicle [2]. As we know, the commercial separator is usually composed of polyethylene (PE) or polypropylene (PP) with double layers or tri-layers. The polymer nature of such separator traps them suffering from bad thermal stability, especially under short-circuit or thermal shock condition [3].

In order to improve the drawback of bare PP or PE separator, surface coating with Al_2O_3 [4], SiO_2 [5], ZrO_2 [6], $AlPO_4$ [7], AlF_3 [8], CeO_2 [9] or other ceramic materials [10] is regarded as an efficient route to strength the physical property without consuming much energy density and cost of separator. However, the research interests of such improving route are mainly focusing on preparation of various kinds of surface coating materials rather than dispersant and wetting reagent [11, 12]. To the best of our knowledge, there are little literatures reporting the influence of dispersant and wetting reagent on wettability, thermal stability and electrochemical property of separator in lithium ion batteries. It is well-known that slurry stability of coating material, wettability of electrolyte with separator, and high-temperature baking shrinkage are regarded as critical factors in determining the physical and electrochemical properties of surface coating PE separator [13]. Recently, Xu [14] coated PVDF on the surface of PP separator and investigated its application in aqueous lithium ion batteries. Thermal shrinkage ratio of separator was decreased from 59.4% to 12.7% in accompany with reduced interface resistance as well as increased ionic conductivity, which were attributed to the PVDF coating layer. Lee [15] coated α-Al_2O_3 on PE separator and found that with the smaller particle size (D_{50}=0.37 μm), the α-Al_2O_3 coated separator exhibited higher porosity and electrolyte uptake as well as lower thermal shrinkage ratio under lower enthylpy. The role of dispersant and wetting reagent in determining physical and electrochemical properties of coating separator should be paid more attention.

Herein, two kinds of surfactant and four kinds of dispersant were adopted to investigate their influence on slurry viscosity, solid state content of slurry, contact angle of separator with electrolyte, and thermal shrinkage ratio of PVDF-coating PE separator. Compared with bare PE, the PVDF-coating PE separator with perfluorinated octylic acid sodium as dispersant and ethylene bis stearic acid amide as wetting reagent exhibits decreased contact angle, lower viscosity, negative-shift Zeta potential, enhanced thermal stability as well as improved electrochemical properties when applied in lithium ion batteries.

2. EXPERIMENTAL SECTION

2.1. Preparation of PVDF slurry

With total solid state content of 61%, the coating composite slurry was prepared by using carboxymethyl cellulose (CMC) as gelatinizer, perfluorinated octylic acid sodium (POAS) or sodium polycarboxylate SN-5040 (5040) as water-based dispersant, ethylene bis stearic acid amide (ST-83, provided by Sanky Chemicals co.) or polyoxyethylene ether (ST-5070, provided by Sanky Chemicals co.) or sulfated ethoxylated alcohols (W-005, provided by Beijing Lanhaiheishi co.) or sodium alkyl succinate (H-875, provided by Beijing Lanhaiheishi co.)) as wetting reagent, PVDF as coating material,

and acrylonitrile copolymer (BM-288E, provided by Beijing Lanhaiheishi co.) as binder. The above mentioned materials were mixed with a weight ratio of 1.73:1.8:1.24:0.84 for PVDF, ethanol, CMC solution, and BM-288E. The wetting reagent (or dispersant) was firstly mixed with CMC and BM-288E and stirred for 30 min. After that, 5wt% of ethanol and PVDF powder were added into the slurry and stirred for 30 min, respectively. Then, deionized water was added with the help of uniform dispersing machine at 6000r min^{-1} for 25 min. Finally, the sonication was utilized to get well-prepared slurry at 200 W for 20 min.

2.2. Coating separator preparation

The as-prepared slurry was uniformly coated on PE separator (12μm) with one-side coating film in a thickness of 8μm. After that, the coated separator was dried in vacuum oven at 50℃ for 24 h.

2.3. Wettability and thermal stability test

Both bare PE and as-prepared PVDF-coated PE separator were cut into sheets with an identical size of 60mm*30mm to test their area density, contact angle as well as electrolyte uptake ability. Thermal stability was tested with calculating thermal shrinkage ratio of the both separators from the machine direction (MD) and transverse direction (TD) after baking at 120℃ 1h.

2.4. Physical characterization

The surface morphology of PVDF powder, PE separator, and PVDF-coated PE separator was observed with scanning electron microscopy (JSM-6490LV, Japan). The contact angle of separator was detected in the optical contact angle measuring device (SL200B, USA). Particles size distribution was analyzed in a laser particle size analyzer (BT-9300H, China). Zeta potential was tested on a Zeta potential tester (Plus90 Zeta, USA).

2.5. Electrochemical performance test

Galvanostatic charge-discharge (GCD) tests of lithium ion batteries with different kinds of separators were carried out on LAND battery testers using CR2016-type coin cell, in where mesocarbon microbeads (MCMB) electrode was treated as cathode, lithium foil was used as anode and 1 M $LiPF_6$ in ethylene carbonate/dimethyl carbonate/diethyl carbonate (1:1:1, volume ratio) was carried out as organic electrolyte. MCMB electrode slurry was prepared by mixing MCMB powder with super P and polyvinylidene fluoride in a weight ratio of 80:10:10 under the help of N-methyl pyrrolidone as solvent. The as-prepared MCMB slurry was coated on aluminum foil with a thickness of 15 μm and further dried in a vacuum oven at 120℃ for 12 h. The weight mass on each electrode was controlled around 1.5-2mg cm^{-2}. Coin cells were assembled in a glove-box (MBRAUN LABstar pro, Germany) with the oxygen and moisture ≤ 0.5 PPM in high-pure argon atmosphere. Before GCD tests, coin cells were set for resting

12 h at room temperature to guarantee the well penetration of electrolyte into electrode. Electrochemical impedance spectroscopy was performed on an Autolab electrochemical station (Autolab 302N, Herisau, Switzerland) in the frequency range of 10^5-10^{-1}Hz with AC voltage of 5mV.

3. RESULTS AND DISCUSSION

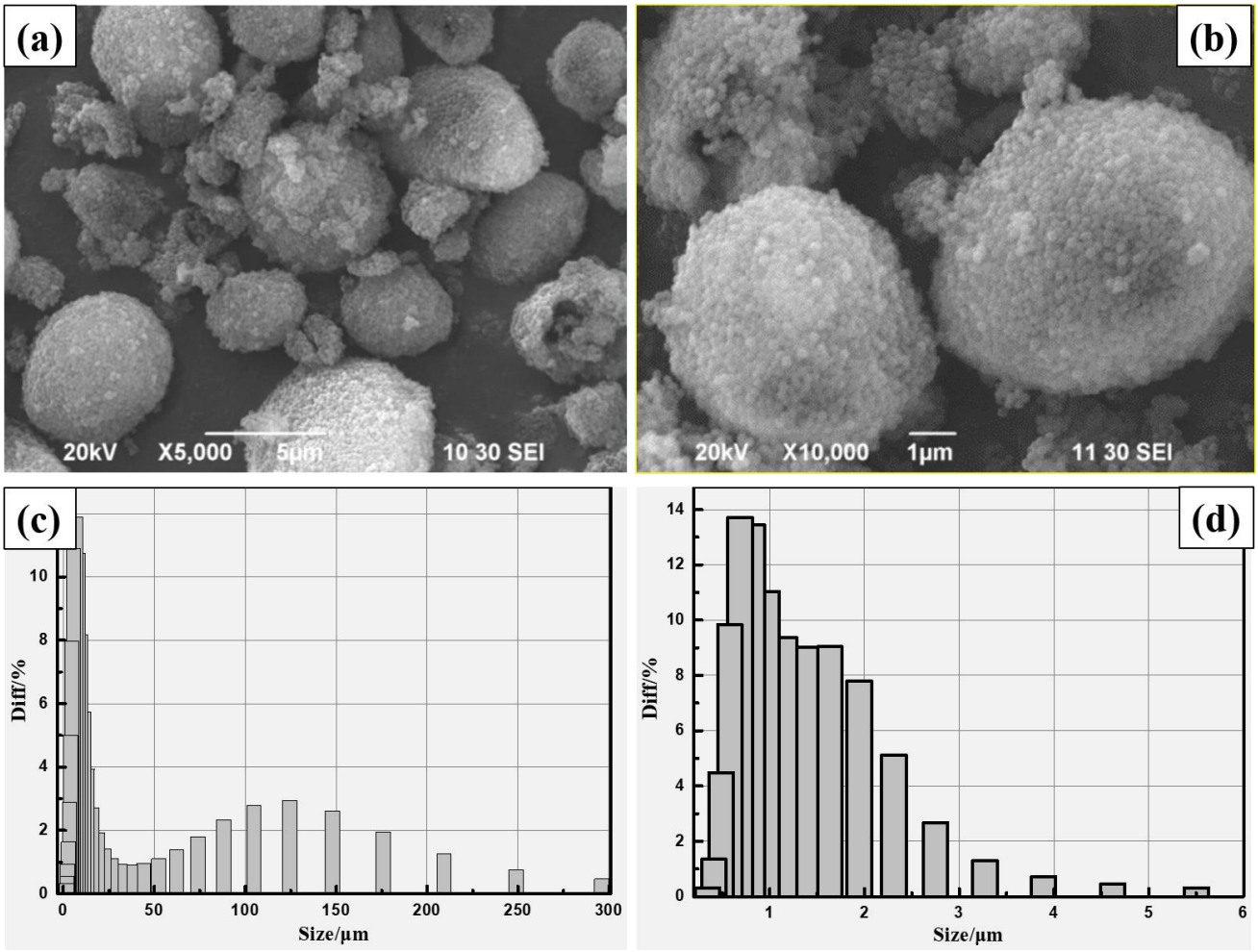

Figure 1. (a-b) SEM images of PVDF powder. Particle distribution pattern of PVDF (c) before and (d) after uniform dispersion

Figure 1 (a-b) shows the SEM image of nano-size PVDF powder used in the coating experiment. It can be observed that the PVDF powder aggregates severely and this observation keeps consistence with the result of particle size distribution, as shown in Figure 1(c). The particle size is in the scale of 100-150μm and the aggregation is composed of smaller particles in the size of 4-10μm, which is believed to be unsuitable for next coating step since a thinner coating layer is helpful to achieving greater energy density of batteries [16]. Thus, we adopted uniform dispersion machine to destroy the particle aggregation and achieved uniform particle distribution in the main range of 700nm (Figure 1(d)), which is feasible to be used in next coating process.

Table 1. the influence of different amount of POAS dispersant on Zeta potential, particle size, viscosity, solid state contents of PVDF slurry

POAS amount/%	0	0.01	0.03	0.05	0.07	0.1
Zeta potential /mV	-30.30	-58.54	-55.36	-55.16	-59.90	-56.39
Particle size /nm	758.4	483.2	356.5	467.4	341.9	322.6
Viscosity /mpa.s	518.4	509.3	504.3	501.7	490.5	498.3
Solid State Content/%	1.071	0.77	0.45	0.42	0.43	0.85

Table 2. the influence of different amount of 5040 dispersant on Zeta potential, particle size, viscosity, up-layer solid state content, down-layer solid state content and gap between up-layer and down-layer of PVDF slurry

5040/%	0	0.1	0.3	0.5	0.7	1.0
Zeta Potential /mV	-30.30	-59.54	-59.36	-58.16	-57.90	-55.39
Particle size /nm	758.4	324.0	318.5	408.9	358.8	381.1
Viscosity /mpa.s	518.4	549.3	604.3	591.7	481.0	578.4
Up-layer Solid State Content/%	12.04	13.17	12.96	12.85	13.33	13.05
Down-layer Solid State Content/%	13.75	13.34	13.12	13.15	13.46	13.30
Gap between up-layer and down-layer/%	1.071	0.17	0.16	0.30	0.13	0.25

Once achieving ideal particles, the preparing PVDF-slurry with different usage amount of two dispersants was investigated in detail. Table 1 and 2 compare the effect of different amounts of POAS dispersant and 5040 dispersant on the zeta potential, particle size, viscosity, as well as solid state content of PVDF slurry, respectively. The particle size results show that bare PVDF slurry mainly focus on 836.9nm while the value of the slurry with 0.3w% of 5040 reaches 318.5nm and the value with POAS one reaches 341.9nm at 0.07wt% of corresponding usage amount. Simultaneously, with the increase of POAS amount, its surface adsorption amount on PVDF gradually increases, which results in the increase of space impeding and the negative shift of Zeta potential. After the adsorptive amount reaches the maximum value, the over-amount PVDF molecular could react with each other to affect the stability of slurry, resulting in the reversely shift of Zeta potential. On the other hand, the solid state content gradually decreases with the increase of dispersant amount, which could be explained by the anoic surfactant nature of 5040. The $CHOO^-$ ion formed after decomposition of 5040 can attach on the surface of PVDF particle and form positive-charging layer, which hampers the aggregation of PVDF [17]. It is concluded that when the usage amount of POAS reaches 0.07wt% or the usage amount of 5040 reaches 0.3wt%, we can get the best particle distribution of slurry. In the following section, we will choose 0.3wt% 5040 or 0.07wt% POAS as dispersant if there is no particular notice.

Contact angle and wettability of separators with different amount of wetting reagents are shown in Figure 2. When compared with bare PVDF-coated separator, PVDF-coated separators with wetting reagents presents improved wettability. Different usage amount of wetting reagent will result in different

extent of wettability, however, contact angle reversely towards lower angle trendy with the increase of wetting reagent. For bare PVDF-coated separator, contact angle reaches 112.2° while PVDF-coated counterpart involved by 0.2wt% ST-83 reaches 31.9°. When using 0.4wt% ST-5070 as wetting reagent, contact angle decreases to the lowest value of 32.7°.

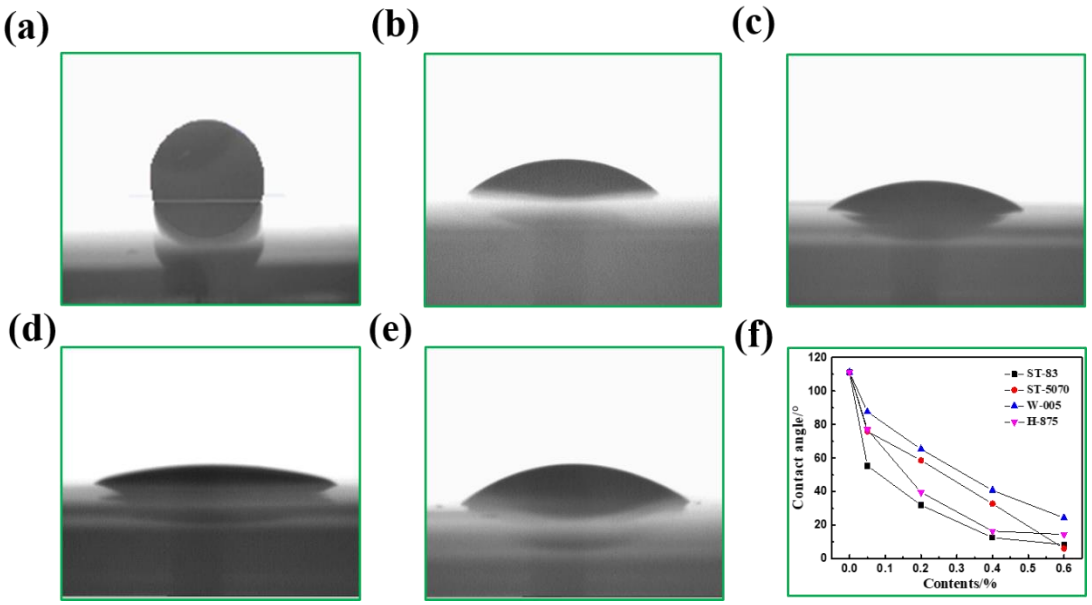

Figure 2. The contact angle with (a) 0%, (b) 0.2 wt% ST-83, (c) 0.4 wt% ST-5070, (d) 0.4 wt% W-005, (e) 0.4 wt% H-875, (f) contact angle with different amount of wetting reagents including ST-83, ST-5070, W-005 and H-875

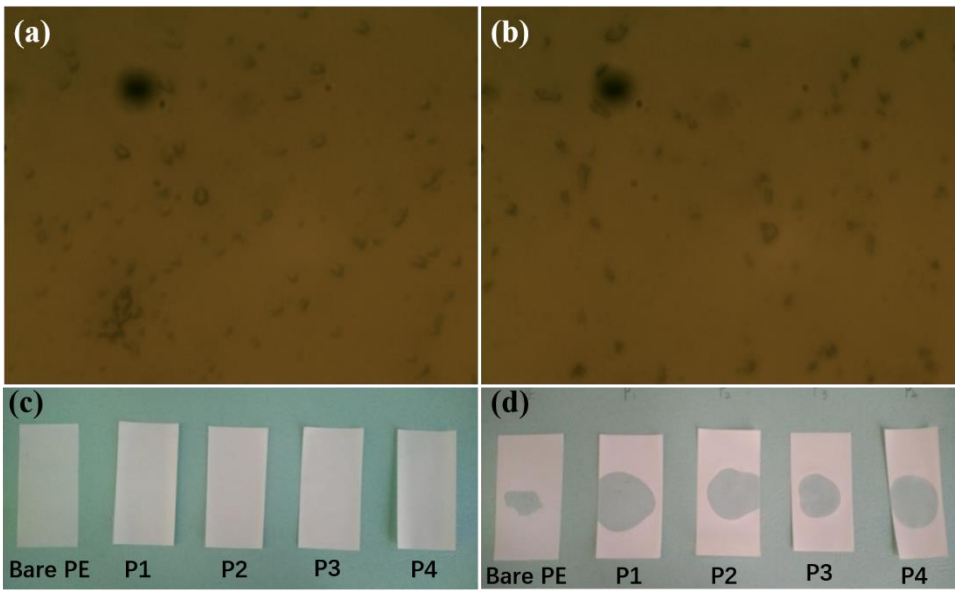

Figure 3. Metallurgical microscopy of (a) bare PVDF slurry and (b) the P2 slurry; The electrolyte wettability (c) before and (d) after dropping electrolyte on bare separator and P1-P4 separators.

For mixing wetting reagent of H-875 and W-005, contact angle reaches 40.7° when the mixing

amount is less than 0.4wt%. It is interesting that when the usage amount of all wetting reagents beyond the proper value, contact angle turns into a lower value but probably with the cost of slurry penetrating across the separator, which also results in the poor coating efficiency. Thus, the PVDF-coating separator can reach superior wetting efficiency when using 0.2wt% ST-83 or 0.4wt% ST-5070 as additive. In the following section, we choose 0.2wt% ST-83 and 0.4wt% ST-5070 as wetting reagent if there is no particular notice.

Herein, in order to further investigate the synergistic effect between surfactant and wetting reagent, we designed four kinds of reagent units: (P1) 0.3wt% 5040 and 0.2wt% ST-83; (P2) 0.07 wt% POAS and 0.2wt% ST-83; (P3) 0.07 wt% POAS and 0.4wt% ST-5070 and (P4) 0.3wt% 5040 and 0.4wt% ST-5070. To make easily understanding, we only use the abbreviation series of P1， P2, P3 and P4 to name the four reagent units, respectively.

Figure 3(a) and (b) further demonstrate the images of metallurgical microscopy of bare slurry and the P2 slurry. It is observed that for the P2 slurry, there is no significant aggregation of PVDF particles and the well-distribution of PVDF particles has been well achieved. However, for bare slurry, PVDF aggregation is observable. Moreover, electrolyte uptake ability of separator before/after using dispersant and wetting reagent has been further evaluated, as shown in Figure 3 (c) and (d). In testing, 50ul of $LiPF_6$ electrolyte was dropped onto the surface of bare separator and PVDF-coated separator. Results of the comparison clearly show that the electrolyte uptake ability of P2 sample is comparable with or even better than other four samples. The expended cover area of electrolyte on separator prepared by adding dispersant and wetting reagent strongly confirms the improved separator wettability.

Table 3 compares the results of electrolyte uptake ability and thermal shrinkage phenomenon of separator under different condition. The addition of dispersant and wetting reagent can shift contact angle towards negative direction, improve slurry stability as well as reduce slurry viscosity. The gap between up-layer solid state content and down-layer solid state content also confirms this reduced trend, further proving the great improvement of slurry stability.

Table 3. Zeta potential, viscosity, gap between up-layer and down-layer solid state content and contact angle of different separators items including bare PE and P1-P4

Testing Items	Testing samples			
	P1	P2	P3	P4
Zeta potential /mV	-59.36	-60.53	-58.61	-58.93
Viscosity /mpa.s	49.5	41.5	39.5	39.5
Gap between Up-layer and Down-layer /%	4.34	3.95	3.62	4.20
Solid state content /%	14.12	13.10	13.68	13.93
Contact angle θ /°	32.99	39.95	38.94	38.34

Table 4. Average loading mass and area density of different separator items including bare PE and P1-P4

Testing items	Bare PE	Testing samples			
		P1	P2	P3	P4
Average mass M/g	0.0137	0.0221	0.0226	0.0229	0.0231
Areal density ρ/g·m^{-2}	7.61	12.28	12.56	12.72	12.83

The area density of coated separator was evaluated with the mass weighting after cutting into the size of 60mm*30mm; From the Table 4, average area density of PVDF-coating separators reaches 12.5g m^{-2}, which is greater than that of bare PE separator (7.6g m^{-2}). The PVDF coating layer with 8μm thickness can make the thickness of separator increase to 1.67 times in accompany with the increase of weight to two times at least. The increased thickness and weight after coating PVDF may decrease the usage amount of electroactive material, which could lead to the decrease of energy density. Thus, the choice of appropriate coating thickness and assembling extent are important. Furthermore, the electrolyte uptake ability of all PVDF-coating PE separators was summarized in Table 5.

Table 5. Electrolyte uptake ability (Average mass variation) of different separator items including bare PE and P1-P4

Items	Average mass before electrolyte dropping /g	Electrolyte dropping /g	Electrolyte uptake /g.m^{-2}
Bare PE	0.0232	0.0095	5.27
P1 /g	0.0556	0.0249	13.83
P2 /g	0.0553	0.0274	15.22
P3 /g	0.0422	0.0247	13.72
P4 /g	0.0427	0.0242	13.44

It is noted that after electrolyte dropping, the PVDF-coating PE separator can take three times of electrolyte volume than that of bare PE separator. The main adsorption section of electrolyte can be ascribed to the PE coating layer. The increment of electrolyte amount can reduce the extent of electrolyte polarization and side reactions during charge-discharge test [7, 18]. Besides area density and electrolyte uptake ability, thermal shrinkage of separator after PVDF-coating was also evaluated in Table 6 to compare thermal stability, which is another important parameter in determining the quality of separator. From the results, it is concluded that the shrinkage ratio of bare PE separator in TD direction and MD direction reaches 7.3% and 8.3%, respectively, while the PVDF-coating PE (P1-P4) separators show 6.0%, 5.0%, 6.7% and 6.0% from TD direction and 6.5%, 6.3%, 6.3% and 7.5%, respectively. The PVDF-coating separator with reduced thermal shrinkage ratio can efficiently impede the extent of short-circuit, improve the high-temperature tolerance ability and enhanced the safety of lithium ion batteries [19].

Table 6. Thermal shrinkage parameters and shrinkage ratio of different separator items from both TD and MD

Separator items	TD/mm	MD/mm	TD thermal shrinkage /%	MD thermal shrinkage/%
Bare PE	27.8	55.0	7.3	8.3
P1	28.2	56.1	6.0	6.5
P2	28.5	56.2	5.0	6.3
P3	28.0	56.2	6.7	6.3
P4	28.2	55.5	6.0	7.5

Figure 4 compares the surface morphology of bare PE and PVDF-coating PE separator with P2. It is observed that bare PE shows tremendous pores in different sizes while PVDF-coating PE with P2 shows more uniform distribution of particles in the size of 0.2-1μm even there is a slight aggregation. Moreover, some detectable slightly gaps between PVDF particles are believed in favor of electrolyte penetration and electrolyte uptake, which can significantly improve the drawbacks of bare PE [20].

Rate capability and cycling stability of battery with bare PE and PVDF-coated PE separators (P1-P4) were investigated in detail. In comparison, when five samples were tested at 0.1C, 0.2C, 0.5, 1C and recovered to 0.1C, the battery with PVDF-coating PE separator with P2 shows higher rate capability (235.6mAh g^{-1} at 1C) than that of the battery with bare PE separator (154mAh g^{-1} at 1C), as shown in Figure 5(a). Moreover, the rate recovering ability of battery with PVDF-coating PE separator with P2 separator reaches 99.1%, much higher than that of battery with bare PE separator (95.1%) when the rate recovers to 0.1C. The cycling stability of batteries with different condition was provided in Figure 5(b). After cycling at 0.5C over 50 cycles, bare PE-based battery only possesses 123.2mAh g^{-1} of specific capacity while the battery based on PVDF-coated counterpart with P2 can deliver 304.2mAh g^{-1} of specific capacity with the capacity retention reaching 51.1% and 93.2%, respectively. The PVDF-coating separator after synergistic introduction of dispersant and wetting reagent can enhance electrolyte uptake ability, reduce interface polarization, improve ionic conductivity and achieve high-rate capability [21, 22].

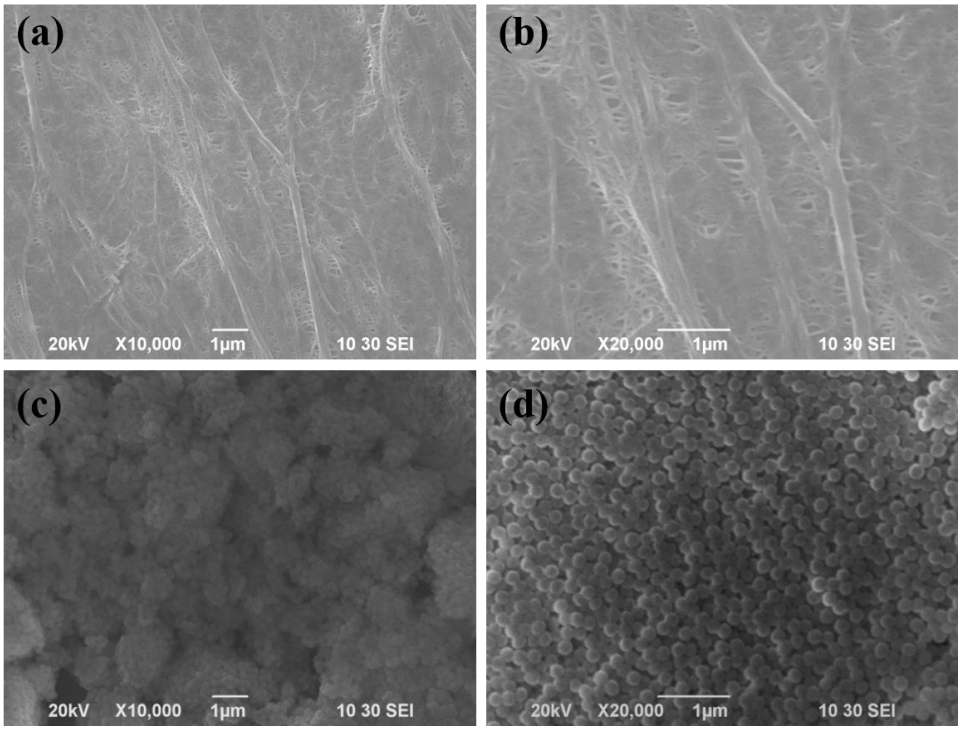

Figure 4. SEM images of (a-b) bare PE separator; (c-d) PVDF-coating PE separator (P2)

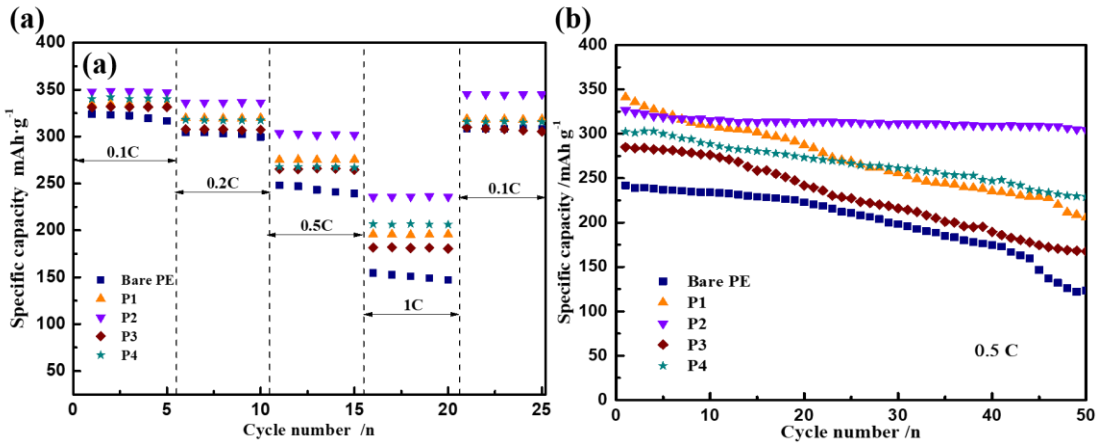

Figure 5. (a) Rate capability and (b) 0.5C rate cycling stability of batteries with bare PE and P1-P4 samples

In order to further illustrate the over-charging (OC) tolerance of separator, the GCD profiles of batteries with different PVDF-coating condition are presented in Figure 6. For bare PE, there is negligible or detectable specific capacity after OC test, strongly confirming the poor safety issue of bare PE separator. However, after PVDF-coating, whatever using any kinds of dispersant and wetting reagent, the GCD profiles after OC test almost keep identical charge/discharge profiles as that of the profiles before OC test. In detail, the specific capacity can recover to 85.7%, 84.9%, 89.2% and 91.2% of its initial specific capacity before OC test for P1, P2, P3 and P4 sample, respectively.

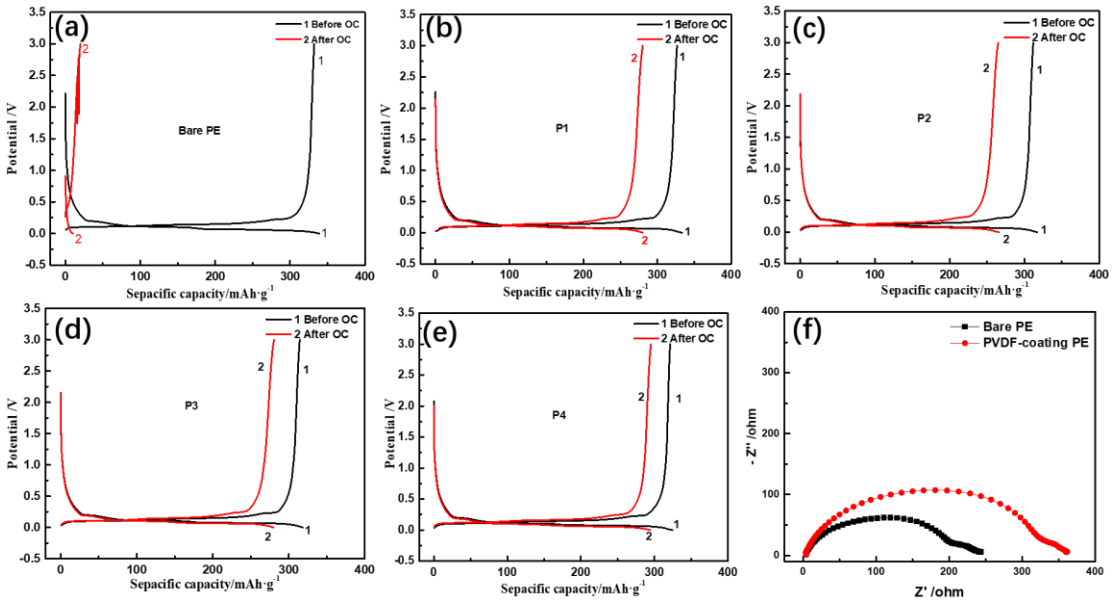

Figure 6. GCD profiles of (a) bare PE, (b) P1, (c) P2, (d) P3 and (e) P4 separator before and after overcharging to 4.6V (OC). (f) EIS pattern of bare PE and PVDF-coating PE (P2)

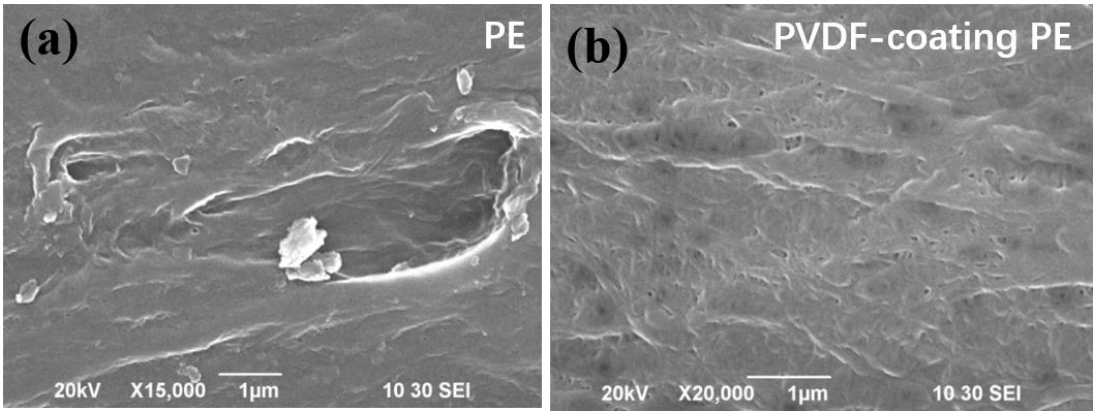

Figure 7. SEM image of bare PE and PVDF-coating PE separator (P2)

In addition, the EIS pattern of PVDF-coating PE (P2) clearly illustrates the increment of charge-transfer resistance (321Ω) compared with bare PE (201Ω), which associates with enhanced electrochemical reaction resistance caused by the thicker separator after surface coating PVDF (Figure 6(f)). Even considering there is a slightly difference of discharge capacity, the trend in combination with rate capability and cycling stability can strongly confirm the conclusion that the best choice in preparation of PVDF-coating slurry is P2 composite which is composed of 0.07wt% POAS as dispersant and 0.2wt% ST-83 as wetting reagent.

Surface morphology of separators after OC test was finally examined to check the effect of surface coating, as shown in Figure 7. It is observed that bare PE separator shows observable micro-size pores on the surface while there are no detectable pores for PVDF-coating PE separator (P2). The existed pores may cause by the penetration of Li-dendrite crossing the separator during the OC test. The PVDF layer can efficiently prevent this phenomenon and function as safety protector during the abuse condition of lithium ion batteries, which keeps consistence with previous physical and electrochemical performances. To further confirm the conclusion that the micro-pore is caused by Li-dendrite, after OC test, we washed all separators with dimethyl carbonate (DMC) and deionized water in series and tested the pH value of the water.

Table 7. pH value of deionized water after washing different kinds of separators dissembled from over-charged batteries

Separator type	pH(25℃)
Bare PE	10.43
P1	7.86
P2	7.77
P3	8.05
P4	8.88

As shown in Table 7, the pH value of bare PE separator reaches 10.43 while the PVDF-coating separators only deliver 7.86, 7.77, 8.05 and 8.88 of pH value for P1, P2, P3 and P4, respectively. The high pH value can be attributed to the formation of Li-dendrite, which transforms into lithium hydroxide after washing with deionized water.

In summary, when compared with previous literatures about the surface coating strategy to improve physical and electrochemical properties of PE separator, this study exquisitely designs a combined additive with dispersant and wetting reagent in preparation of coating-material slurry. For example, in previous research literatures, the researchers mainly focused on the influence of different surface coating materials on the electrochemical properties of PE separator including $MgAl_2O_4$[23], Sb_2O_3[24] or polar methyl acrylate monomer[25]. Besides, in Maryam's study[26], the author utilized sodium polymethacrylate as dispersant to investigate its influence on physical properties of TiO_2/PVDF separator. The simple consideration of dispersant or wetting reagent could result in the isolated and unilateral conclusion about the role of additive. Simultaneously, to the best of our knowledge, the relative research on synergistic effect of dispersant and wetting reagent has seldom been reported and should be paid more attention since it is important in preparation of high quality slurry. In this study, we proposed a comprehensive route to combine the advantages of dispersant and wetting reagent to prepare PVDF-based PE separator, which could accelerate the research and industrial implementation progress of coating separator for high-performance lithium ion batteries.

4. CONCLUSION

In this research, two kinds of dispersant and four kinds of wetting reagent were combined together to investigate their synergistic effect on physical and electrochemical properties of PE separator in lithium ion batteries. The best combination route is to use perfluorinated octylic acid sodium as dispersant and ethylene bis stearic acid amide as wetting reagent. The addition of perflurorinated octylic acid sodium can improve electrolyte uptake ability, reduce interface polarization, enhance overcharge tolerance of separator, thus improving the electrochemical high rate capability and cycling stability. While the application of ethylene bis stearic acid amide can decrease the interfacial tension, reduce the contact angle between electrolyte and electrode, and remarkably utilize the electrochemical active sites. The adopted suitable dispersant and wetting reagent plays an importantly synergistic role in achieving well-coated PVDF-based separator for high safety lithium ion batteries.

ACKNOWLEDGEMENT
This work was financially supported by the Key R&D and Promotion Projects (Science and Technology Key Projects) of Henan Province (Grant No. 192102210079), basic research project of the Key scientific research project of the higher education institutions of Henan Province of China (Grant No. 20ZX008), Doctoral foundation of Zhengzhou University of Light Industry (No. 2017BSJJ043) and Project of Science and Technology Activities of College Students in Zhengzhou University of Light Industry (Grant No. 2020-LX-312).

References

1. M. Li, J. Lu, Z. Chen, K. Amine, *Adv. Mater.*, 30 (2018) e1800561.

2. P.V. Chombo, Y. Laoonual, *J. Power Sources.*,478 (2020) 228649.
3. K. Park, J.H. Cho, K. Shanmuganathan, J. Song, J. Peng, M. Gobet, S. Greenbaum, C.J. Ellison, J.B. Goodenough, *J. Power Sources*, 263 (2014) 52.
4. Z. Qiu, S. Yuan, Z. Wang, L. Shi, J.H. Jo, S.-T. Myung, J. Zhu, *J. Power Sources*, 472 (2020) 228445.
5. J. Hu, Y. Liu, M. Zhang, J. He, P. Ni, *Electrochim. Acta*, 334 (2020) 135585.
6. L. Liu, Y. Wang, C. Gao, C. Yang, K. Wang, H. Li, H. Gu, *J. Membr. Sci.*, 592 (2019) 117368.
7. S. Ma, H. Lin, L. Yang, Q. Tong, F. Pan, J. Weng, S. Zheng, *Electrochim. Acta.*, 320 (2019) 134528.
8. W.-K. Shin, J.-H. Yoo, D.-W. Kim, *J. Power Sources*, 279 (2015) 737.
9. X. Luo, Y. Liao, Y. Zhu, M. Li, F. Chen, Q. Huang, W. Li, *J. Power Sources*, 348 (2017) 229.
10. M. Zhu, Q. Wang, H. Zhou, L. Qi, *Energy Technol.*, 8 (2020) 2000228.
11. Z. Wang, P. Pang, Z. Ma, H. Chen, J. Nan, *J. Electrochem.Soc.*, 167 (2020) 090507.
12. X. Sun, W. Xu, X. Zhang, T. Lei, S.-Y. Lee, Q. Wu, *J. Energy. Chem.*, 52 (2021) 170.
13. H. Zheng, Z. Wang, L. Shi, Y. Zhao, S. Yuan, *J. Colloid Interface Sci.*, 554 (2019) 29.
14. R. Xu, X. Huang, X. Lin, J. Cao, J. Yang, C. Lei, *J. Electroanal. Chem.*, 786 (2017) 77.
15. D.-W. Lee, S.-H. Lee, Y.-N. Kim, J.-M. Oh, *Powder Technol.*, 320 (2017) 125.
16. P. A, Z. Zhang, *Chem. Rev.*, 104 (2004) 4419.
17. X. Liang, Y. Yang, X. Jin, Z. Huang, F. Kang, *J. Membr. Sci.*, 493 (2015) 1.
18. F. Zhang, X. Ma, C. Cao, J. Li, Y. Zhu, *J. Power Sources*, 251 (2014) 423.
19. H. Liu, J. Xu, B. Guo, X. He, *Ceram. Int.*, 40 (2014) 14105.
20. S. Ali, C. Tan, M. Waqas, W. Lv, Z. Wei, S. Wu, B. Boateng, J. Liu, J. Ahmed, J. Xiong, J.B. Goodenough, W. He, *Adv. Mater. Interfaces*, 5 (2018) 1701147.
21. Y.-S. Lee, Y.B. Jeong, D.-W. Kim, *J. Power Sources*,195 (2010) 6197.
22. Y.H. Liao, X.P. Li, C.H. Fu, R. Xu, L. Zhou, C.L. Tan, S.J. Hu, W.S. Li, *J. Power Sources*, 196 (2011) 2115.
23. M. Raja, K. Bicy, S. Suriyakumar, N. Angulakshmi, S. Thomas, A. M. Stephan, *Ionics*, 24 (2018) 3451.
24. L.J. Wang, Z.H. Wang, Y. Sun, X. Liang, H.F. Xiang, *J. Membrane. Sci., 572 (2019) 512.*
25. L. Sheng, L. Song, H. Gong, J.J. Pan, Y.Z. Bai, S.J. Song, G.J. Liu, T. Wang, X.L. Huang, J.P. He, *J. Power Sources*,479 (2020) 228812.
26. M. Tavakolmoghadam, T. Mohammadi, *Polym. Eng. Sci*, (2019) Doi: 10.1002/pen

© 2021 The Authors. Published by ESG (www.electrochemsci.org). This article is an open access article distributed under the terms and conditions of the Creative Commons Attribution license (http://creativecommons.org/licenses/by/4.0/).